Oliver-Meseguer, J.; Boronat Zaragoza, M.; Vidal Moya, JA.; Concepción Heydorn, P.; Rivero-Crespo, MÁ.; Leyva Perez, A.; Corma Canós, A. (2018). Generation and Reactivity of Electron-Rich Carbenes on the Surface of Catalytic Gold Nanoparticles. Journal of the American Chemical Society. 140(9):3215-3218. https://doi.org/10.1021/jacs.7b13696

Generation and reactivity of electron–rich carbenes on the surface of catalytic gold nanoparticles

Judit Oliver–Meseguer,† Mercedes Boronat,† Alejandro Vidal–Moya,† Patricia Concepción,† Miguel Ángel Rivero–Crespo,† Antonio Leyva–Pérez,*,† and Avelino Corma.*,†

†Instituto de Tecnología Química (UPV-CSIC), Universitat Politècnica de València-Consejo Superior de Investigaciones Científicas, Avda. de los Naranjos s/n, 46022 Valencia, Spain.

Supporting Information Placeholder

ABSTRACT: The reactive nature of carbenes can be modulated, and ultimately reversed, by receiving additional electron density from a metal. Here, it is shown that Au nanoparticles (NPs) generate an electron–rich carbene on surface after transferring electron density to the carbonyl group of an in–situ activated diazoacetate, as assessed by Fourier transformed infrared (FT–IR) spectroscopy, magic angle spinning nuclear magnetic resonance (MAS NMR) and Raman spectroscopy. Density functional theory (DFT) calculations support the observed experimental values and unveil the participation of at least three different Au atoms during carbene stabilization. The surface stabilized carbene shows an extraordinary stability against nucleophiles, and rather react with electrophiles to give new products. These findings showcase the ability of catalytic Au NPs to inject electron density in energetically high but symmetrically allowed valence orbitals of sluggish molecules.

Carbenes are divalent C–atoms, often generated in–situ with catalytic metals to program their reactivity towards nucleophiles.[1] However, carbenes can reverse their reactivity if the catalytic metal transfers a significant amount of electron density to unoccupied bonding orbitals. This has been achieved so far by spontaneous one electron oxidation of soluble Co^{2+} and $Fe^{2+/0}$ carbene complexes.[2] The latter feature suitable quasi–planar ligands that not only furnish an appropriate chemical environment for the electron–rich carbene, but also provide the energetically and spatially suitable valence orbitals to engage the empty anti–bonding orbitals of the carbene, since a direct electron transfer from the metal to the carbene is severely restricted. It would be of interest to have metals able to do so on solid surfaces, thus enabling heterogeneous catalysis and avoiding ligands.

Au is able to bind carbenes as a metal complex in solution and also as NPs.[3-5] The latter reacts in a classical way, probably on unsaturated Au atoms present in the boundaries, corners and vertexes of the NP.[5] It may occur that bulk Au atoms would inject electron density into the symmetrically matching unoccupied valence orbitals of a suitable carbene, if efficiently formed on the NP surface. This is not more what occurs during the activation on Au NPs of relatively inert molecules such as H_2,[6] O_2,[7] HCl[8] and benzenes and alkynes,[9] which coordinate on unsaturated Au atoms and then receive electron density from the NP bulk. The electron–rich intermediates are stable enough to be detected[8] and used in productive catalytic processes.[6-9]

Figure 1 shows the temperature programmed FT–IR spectrum of a sample of commercially–available, homogeneously dispersed 3 nm Au NPs on TiO_2 (1 wt%), degassed at 200 ºC under vacuum, and treated with ethyl diazoacetate (EDA, **1**) at 25 ºC. According to blank experiments with **1** adsorbed on TiO_2 (Fig S1-3), the peaks at 2115 and 1640 cm^{-1} corresponds to unreacted **1**, and the peaks at 1736, 1679 and 1568 cm^{-1} correspond to the hydration product ethyl glycolate **2**, as also assessed by the disappearance of hydroxyl groups of Au–TiO_2 after adsorption of **1**. However, new peaks at 1704 and 1549 cm^{-1} rise in intensity after **1** dosing, remaining quite stable to evacuation. These peaks can be ascribed to the strongly blue–shifted C=O of an electron–rich carbene that receives electron density from Au (1549 cm^{-1}, **3A**)[10] and the free C=O of a classical Au carbene (1704 cm^{-1}, **3B**).[11] Increasing temperature to 150 ºC triggers formation of ethyl fumarate and ethyl maleate **4**, as assessed by the peaks at 1711, 1667 and 1524 cm^{-1} (see Fig S2).[1b] Benzyl diazoacetate gives also blue–shifted C=O signals in the presence of Au–TiO_2 (Fig S3).

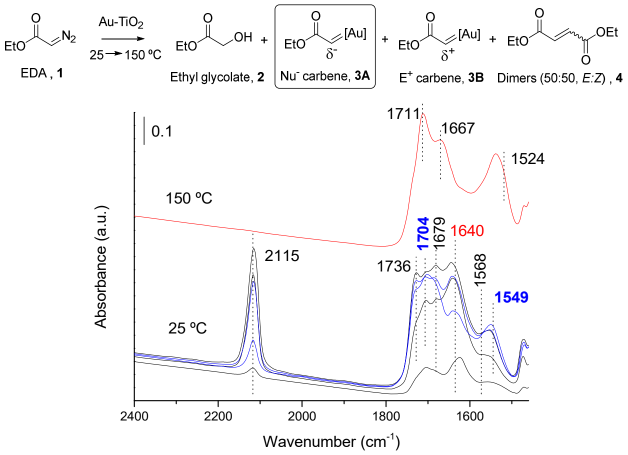

Figure 1 Temperature programmed FT–IR spectra of **1** adsorbed on Au–TiO_2 at increasing dosing (black lines), after evacuation at 10^{-6} mbar (blue lines) at 25 ºC, and after increasing temperature to 150 ºC (red line).

Figure 2A shows the ^{13}C CP/MAS NMR spectra of isotopically labelled $EtOOC^{13}CHN_2$ (**1**–^{13}C),[12a] adsorbed on Au–TiO_2 (surface Au atoms/**1** =1), and sealed in an ampule (see Fig S4 for full spectra). The mixture at RT shows the original signal of **1**–^{13}C centered at 46 ppm (Fig S4) together with three new signals centered at 41, 77 and 132 ppm (broad), the two latter corresponding to **2** and **4**, respectively. Notice that, under these conditions, the dimerization reaction has been completed. After heating at 80 ºC during 30 min, the signal of **1**–^{13}C completely disappears and the signal ranging from ~30 to ~50 ppm, with a maximum at 41 ppm, persists, without further changes in the spectrum for longer heating times. Notice that surface heterogeneity broadens signals in the spectrum. A very recent work[4] reports a nucleophilic Au carbene complex resonating at 18.2 ppm in ^{13}C liquid NMR, which strongly suggests that the signal at 41 ppm may correspond to an electron–rich C carbene atom. Please note that a carbene can persist after heating since the experiment is made in the gas phase with very low covering level, thus bimolecular reactions are hampered. **1**–^{15}N was also prepared[12b] and co-adsorbed with **1**–^{13}C, and the combined ^{15}N and ^{13}C CP/MAS NMR spectra confirm that the peak at 41 ppm only forms after N_2 release (Fig S5). Please notice the difficulties associated in characterizing nucleophilic metal carbenes by NMR, since they usually feature paramagnetic metals.[2,12c] Figure 2B shows the corresponding time–resolved Raman spectra, and two new peaks at ~290-320 and 445 cm^{-1} appear, which could be assigned to Au-C and Au-O vibrations of carbenes **3**, respectively, beside the Raman bands at 197, 396, 514 and 639 cm^{-1} corresponding to TiO_2.

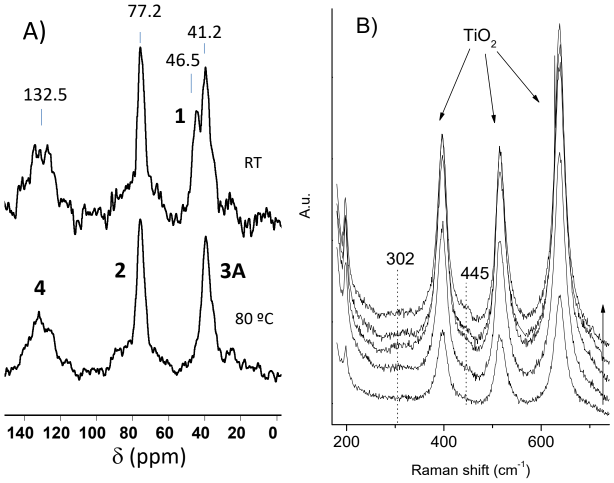

Figure 2 A) ^{13}C CP/MAS NMR spectra of Au–TiO_2 loaded with **1** (Au/**1**= 5) at RT (top) and after heating at 80 ºC for 30 min (bottom). Spectrometer frequency is 100.6 MHz and spinning rate is 5 kHz. B) Raman spectra of **1** adsorbed on Au–TiO_2 at RT and evolution with time (24, 35, 46, 74 and 86 min).

Figure 3 shows the calculated interaction energies, net atomic charges, bond lengths, νCO and RAMAN frequencies, and NMR values of carbene **3** adsorbed on a Au_{10} model, with either the oxygen atom of the carbonyl (A) or ester (B) groups attached to the surface Au atoms. Remarkably, the carbene atom bonds to two Au atoms (Au-C-Au) in all configurations, regardless different coordination modes or Au NP arrangements (see Table S1 for additional computed structures). A further stabilization occurs if an O atom coordinates Au, in such a way that the highest interaction energy (-37 kcal mol^{-1}) is achieved when the O atom of C=O coordinates to the Au surface at the relatively small distance of 2.36 Å (structure A). The calculated νCO and Raman frequencies, and NMR shifts for the carbene C atom in structure A, 1578, 407 and 305 cm^{-1}, and 21 ppm, respectively, are close to those observed experimentally (1537, 445, 302 cm^{-1} and 41 ppm), much closer than any other computed structure (see Table S1 and also Table S2 for related reported values).[4,10] The C=O bond length changes from 1.22 to 1.24 Å in structure A, with a ca. 20% increase of neat negative charge at the O atom and a similar increase of neat positive charge at the C atom, which unambiguously indicates the weakening of the C=O bond. Finally, the net and total charges summarized in Fig. 3 and Fig. S5 show that there is a transfer of ~ 0.5e$^-$ from Au to the adsorbed carbene, causing an increase in the net negative charge on the carbene atom of 0.7–0.8 e (see Table S3 for validation with B3PW91 and M06 methods).[3b,4] These results, together, strongly support the electronic transfer from the Au surface to the antibonding orbitals of the C=O bond to generate the electron–rich carbene **3A**.

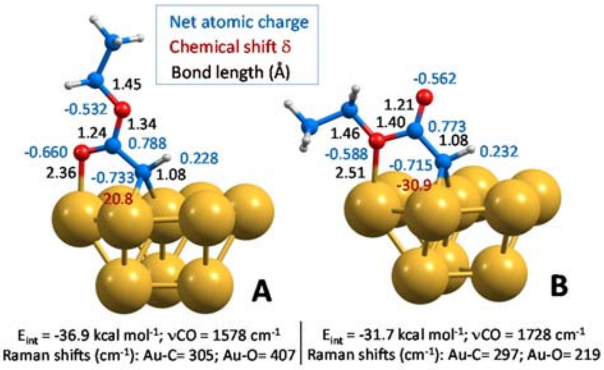

E_{int} = -36.9 kcal mol^{-1}; νCO = 1578 cm^{-1}
Raman shifts (cm^{-1}): Au-C= 305; Au-O= 407

E_{int} = -31.7 kcal mol^{-1}; νCO = 1728 cm^{-1}
Raman shifts (cm^{-1}): Au-C= 297; Au-O= 219

Figure 3 DFT calculations of the most probable configurations of carbene **3** on Au NPs, including bond lengths (black) and net atomic charges (blue).

The Au–TiO_2 (0.1 mol%) catalyzed reaction of **1**, in toluene at 70 ºC, gives an equimolecular mixture of dimers **4**, up to 90% yield.[13] Au–ZnO and Au–Al_2O_3 were also effective, and Au–TiO_2 could be reused up to 10 times without depletion in the final yield of **4**. For all Au NPs, the equation rate for the formation of **4** was $r_0 = k_{exp}[\mathbf{1}][Au]$, which is the expected equation rate for a classical Lewis–acid catalyzed activation and dimerization of **1** (Fig S6).[14a] The Lewis base Bu_3N (0.01 mol%) severely stopped the formation of **4**, while a similar amount of NaI had no effect. Besides, the cross dimerization between ethyl (**1**) and *tert*–butyl diazoacetate, which possess a bulky group that impedes a good coordination on the bulk Au atoms and thus hampers metal catalysis on planar surfaces (Taft effect),[14b] proceeds very well (Fig S7), which supports that **1** transforms to **3B** at unsaturated Au atoms. This process may run in parallel and be co–operative with the formation of **3A** on bulk Au atoms, with an electronic flow from the unsaturated to the bulk (Fig S8).[14c-e] Notice that products in solution differ from species observed by in–situ IR, NMR and Raman techniques, since the latter mainly correspond to species remaining adsorbed on surface (Fig S9).

The reactivity of **3A** and other potential electron–rich Au carbenes was then studied. Table 1 shows the results with Au–TiO_2, Au$^+$ complexes and some representative catalysts. In general, the reactivity of **1** drastically decreases in the presence of Au–TiO_2. For instance, toluene, *n*–hexane and ethanol (entry 1) can be used as a reaction solvent since they do not react in the presence of Au–TiO_2, in clear contrast with Au$^+$ complexes[15,16] and classical metal species.[17–23] The electron–

Table 1 Reactivity of carbene–forming substrates in the presence of different catalysts.

Entry	Reaction[a]	Catalyst / products (catalyst loading, product yield and reference)[b]		
		Au–TiO$_2$	Au$^+$ complexes	Other representative catalysts
1	Insertion reagents $\xrightarrow[70\,^\circ C,\ 24\ h]{\mathbf{1}\ (0.5\ M)}$ **5a-d** Reagent= Toluene, *n*-hexane, ethanol	1–20 mol%, no reaction	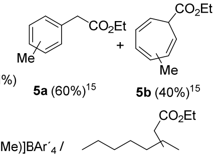 IPrAuCl + NaBAr´$_4$ / (2.5 mol%) **5a** (60%)[15] + **5b** (40%)[15] [IPrAu(NCMe)]BAr´$_4$ / (5 mol%) **5c** (78%, mixt. of isomers)[16]	Rh$_2$(OOCCF$_3$)$_4$ (2 mol%) / **5b** (95%)[17-19] Ag(3,5-(CF$_3$)$_2$PyrPy) (5 mol%) / **5c** (55%, mixture of isomers)[18-20] Rh$_2$(OAc)$_4$ (0.2 mol%) / 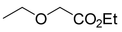 **5d** (88%)[21,22] IPrCuCl (4 mol%) / **5d** (95%)[22,23]
2[c]	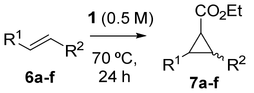 **1** (0.5 M), 70 °C, 24 h **6a-f** → **7a-f**	5 mol%; **7a** (10%), **7b** (27%), **7c-f** (35-24%)	IPrAuCl + NaBAr´$_4$ / **7b** (>95%)[16] (2.5 mol%)	Tp^{Ms}Cu (2 mol%) / **7a-b** (84-99%)[24] IPrCuCl (4 mol%) / **7b** (99%)[23] Co^{2+}-porphyrin (1 mol%) / **7b** (>90%)[25]
3	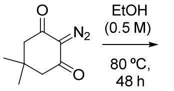 **8** EtOH (0.5 M), 80 °C, 48 h	10-25 mol%, 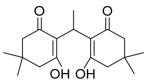 **9** (58-82%)	AuPPh$_3$Cl + AgBF$_4$ (5 mol%) / 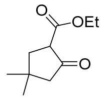 **10** (50%)[14e,28]	Microwaves **10** (96%)[29] hν (450 W) **9** (40%)[31] Rh$_2$(OAc)$_4$ (2 mol%) 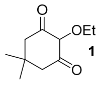 **11** (40%)[30]
4	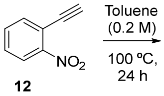 **12** Toluene (0.2 M), 100 °C, 24 h	10 mol%, 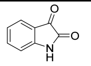 **13** (15%) 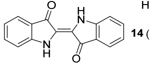 **14** (25%)	AuPPh$_3$Cl + AgNTf$_2$ (5 mol%) / 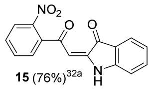 **15** (76%)[32a]	Ir(PPh$_3$)$_2$H(ba) (100 mol%) / 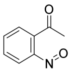 **16** (87%)[32b]

[a] Reaction conditions for Au–TiO$_2$ catalyst, Au–ZnO and Au–Al$_2$O$_3$ catalysts gave similar results in most cases. Blank experiments with Au–TiO$_2$ show only marginal yields of the nucleophile carbene products **7a-d**, **9**, **13** and **14**. [b] See detailed reaction conditions in references. IPr: 1,3–bis(diisopropylphenyl)imidazole–2–ylidene], BAr´$_4$: tetrakis–(3,5–bis(trifluoromethyl)phenyl)borate, PyrPy: 2,2′–pyridylpyrrolide—ligand, Tp^{Ms}: hydrotris(3,5– (2,4,6–trimethylphenyl)pyrazolyl)borate, ba: benzylideneacetone. [c] R^1= *n*-But, R^2= H **6a**; R^1= Ph, R^2= Me **6b**; R^1= 4-R-Ph (R=CF$_3$, Br, H, Me), R^2= H **6c-f**. Mass balances account for >95% in entries 1–3 and c.a. 80% in entry 4

rich nature of **3A** is also seen during the cyclopropanation of alkenes (entry 2). In contrast to classical cyclopropanation reactions where electron–rich alkenes are much more reactive,[16,23,24] **3A** reacts worse with electron–rich 1–hexene **6a** than with electron–poor styrenes **6b–f**, the similar reactivity trend found with Co^{2+} porphyrin radical carbene catalysts.[25] A Hammett plot confirms this tendency (Fig S10). The higher reactivity of the Co^{2+} complex respect Au–TiO$_2$ catalyst correlates with the more electron density transferred by the former (ca. $1e^-$) than by the latter ($0.2e^-$ according to DFT). Different Au–TiO$_2$ samples with average sizes of 7, 12, 17 and 21 nm, respectively, were prepared, characterized,[26] and tested as catalysts for the cyclopropanation of **6d** (Fig S11–15), and the results clearly showed that the cyclopropanation rate increases linearly with the amount of exposed bulk Au atoms in the NP, and not with the amount of unsaturated Au atoms.

Other representative carbene-forming substrates were tested. Dimedone **8**[27] (entry 3) is a typical reagent for Wolff rearrangements or alcohol insertion reactions, which gives cyclopentane **10**[14d,28–29] and ether **11**[30] after intra– or inter–molecular nucleophilic attack to the carbene of **8** in ethanol solvent, respectively, under metal or microwave catalyzed conditions. In clear contrast, coupled bis–dione **9** was the only product obtained with Au–TiO$_2$ catalyst, in up to 82% yield, irrespective of the presence of light or not, and without any trace of Wolff rearrangement or alcohol insertion products. An electron–rich carbene of **8** on Au–TiO$_2$ can be invoked as intermediate of the reaction,[31a,b] since blank experiments showed that Au–TiO$_2$ does not oxidize ethanol to acetaldehyde in the absence of **8** under identical reaction conditions, and a very active aerobic oxidation catalyst of alcohols such as Au–CeO$_2$ gives a similar yield of **9** (57%).[31c]

Ortho–nitro phenylacetylene **12** (entry 4) generates *oxo*–carbenes with metal catalysts, including products **15**[32a] and **16**.[32b] When Au–TiO$_2$ was used as a catalyst, neither **15** nor **16** were formed, but just isatin **13** and indigo dye **14**. These products come from rearrangements and radical oxidation of carbene atoms, as previously observed with Cu^+,[32c] which suggests the formation of electron–rich carbenes of **12**.[32d]

In conclusion, combined experimental and theoretical evidences strongly support that Au NPs generate and stabilize electron–rich carbenes on surface, after electronic transfer to the anti–bonding valence orbitals of the C=O group of RCOCHN$_2$ molecules. This carbene umpolung avoids participation in insertion reactions but rather enables the carbene to act as a nucleophile in addition reactions.[33]

ASSOCIATED CONTENT

Supporting Information

Experimental section, compound characterization and additional Figures S1–15 and Table S1–3. This material is available free of charge via the Internet at http://pubs.acs.org.

AUTHOR INFORMATION

Corresponding Author

E-mail: anleyva@itq.upv.es, acorma@itq.upv.es; phone: +34963877800; fax: +349638 77809.

Notes

The authors declare no competing financial interests.

ACKNOWLEDGMENT

Financial support by MINECO through the Severo Ochoa program, RETOS program (CTQ2014–55178–R) and Ramón y Cajal Program (A. L.–P.) is acknowledged. J. O.–M. thanks ITQ for the concession of a contract. We thank to the Electron Microscopy Service of the UPV.

REFERENCES

(1) a) Werlé, C.; Goddard, R.; Philipps, P.; Farès, C.; Fürstner, A. *J. Am. Chem. Soc.* **2016**, *138*, 3797–3805; b) Fortea-Perez, F. R.; Mon, M.; Ferrando-Soria, J.; Boronat, M.; Leyva-Perez, A.; Corma, A.; Herrera, J. M.; Osadchii, D.; Gascon, J.; Armentano, D.; Pardo, E. *Nat. Mater.* **2017**, *16*, 760–766. For detailed computational studies on gold carbenes and their usual reactivity, see c) dos Santos Comprido, L. N.; Klein, J. E. M. N.: Knizia, G.; Kästner, J.; Hashmi, A. S. K. *Angew. Chem. Int. Ed.* **2015**, *54*, 10336–10340; *Chem. Eur. J.* **2016**, *22*, 2892–2895.

(2) a) Wolf, J. R.; Hamaker, C. G.; Djukic, J.–P.; Kodadek, T.; Woo, L. K. *J. Am. Chem. Soc.* **1995**, *117*, 9194–9199; b) Dzik, W. I.; Xu, X.; Zhang, X. P.; Reek, J. N. H.; de Bruin, B. *J. Am. Chem. Soc.* **2010**, *132*, 10891–10902; c) Lu, H.; Dzik, W. I.; Xu, X.; Wojtas, L.; de Bruin, B.; Zhang, X. P. *J. Am. Chem. Soc.* **2011**, *133*, 8518–8521; d) Russell, S. K.; Hoyt, J. M.; Bart, S. C.; Milsmann, C.; Chantal, S.; Stieber, E.; Semproni, S. P.; DeBeer, S.; Chirik, P. J. *Chem. Sci.* **2014**, *5*, 1168–1174.

(3) For the first gold–catalyzed reaction involving carbene intermediates and a full mechanistic discussion see a) Hashmi, A. S. K.; Frost, Tanja M.; Bats, J. W. *J. Am. Chem. Soc.* **2000**, *122*, 11553–11554 and b) Hashmi, A. S. K.; Rudolph, M.; Siehl, H.–U.; Tanaka, M.; Bats, J. W.; Frey; W. *Chem. Eur. J.* **2008**, *14*, 3703–3708; c) Benitez, D.; Shapiro, N. D.; Tkatchouk, E.; Wang, Y.; Goddard III, W. A.; Toste, F. D. *Nat. Chem.* **2009**, *1*, 482–486; d) Seidel, G.; Fürstner, A. *Angew. Chem. Int. Ed.* **2014**, *53*, 4807–4811; e) Wang, Y.; Muratore, M. E.; Echavarren, A. M. *Chem. Eur. J.* **2015**, *21*, 7332–7339.

(4) Pujol, A.; Lafage, M.; Rekhroukh, F.; Saffon-Merceron, N.; Amgoune, A.; Bourissou, D.; Nebra, N.; Fustier-Boutignon, M.; Mézailles, N. *Angew. Chem. Int. Ed.* **2017**, *56*, 12264–12267.

(5) Carrettin, S.; Blanco, M. C.; Corma, A.; Hashmi, A. S. K. *Adv. Synth. Catal.* **2006**, *348*, 1283–1288.

(6) a) Corma, A.; Serna, P. *Science* **2006**, *313*, 332–334; b) Yang, X.; Kattel, S.; Senanayake, S. D.; Boscoboinik, J. A.; Nie, X.; Graciani, J.; Rodriguez, J. A.; Liu, P.; Stacchiola, D. J.; Chen, J. G. *J. Am. Chem. Soc.* **2015**, *137*, 10104−10107, c) Bond, G. C. *Gold Bull.* **2016**, *49,* 53–61.

(7) a) Huang, J.; Akita, T.; Faye, J.; Fujitani, T.; Takei, T.; Haruta, M. *Angew. Chem. Int. Ed.* **2009**, *48*, 7862–7866; b) Boronat, M.; Leyva–Pérez, A.; Corma, A. *Acc. Chem. Res.* **2014**, *47*, 834–844.

(8) Oliver–Meseguer, J.; Doménech–Carbó, A.; Boronat, M.; Leyva–Pérez, A.; Corma, A. *Angew. Chem. Int. Ed.* **2017**, *56*, 6435 –6439.

(9) a) Corma, A.; Juarez, R.; Boronat, M.; Sánchez, F.; Iglesias, M.; Garcia, H. *Chem. Commun.* **2011**, *47*, 1446–1448; b) Leyva–Pérez, A.; Oliver–Meseguer, J.; Cabrero–Antonino, J. R.; Rubio–Marqués, P.; Serna, P.; Al–Resayes, S. I.; Corma, A. *ACS Catal.* **2013**, *3*, 1865−1873.

(10) Iwakura, I.; Tanaka, H.; Ikeno, T.; Yamada, T. *Chem. Lett.* **2004**, *33*, 140–141.

(11) Penoni, A.; Wanke, R.; Tollari, S.; Gallo, E.; Musella, D.; Ragaini, F.; Demartin, F.; Cenini, S. *Eur. J. Inorg. Chem.* **2003**, 1452–1460.

(12) a) Ranocchiari, M.; Mezzetti, A. *Organometallics* **2009**, *28*, 3611–3613; b) Albertin, G.; Antoniutti, S.; Botter, A.; Castro, J. *Inorg. Chem.* **2015**, *54*, 2091–2093; c) Cantat, T.; Jaroschik, F.; Nief, F.; Ricard, L.; Mézailles, N.; Le Floch, P. *Chem. Commun.* **2005**, 5178–5180.

(13) Zhou, Y.; Trewyn, B. G.; Angelici, R. J.; Woo, L. K. *J. Am. Chem. Soc.* **2009**, *131*, 11734–11743.

(14) a) Hodgson, D. M.; Angrish, D. *Chem. Eur. J.* **2007**, *13*, 3470–3479; b) Fonseca, G. S.; Silveira, E. T.; Gelesky, M. A.; Dupont, J. *Adv. Synth. Catal.* **2005**, *347*, 847–853; c) Bai, D.; Jennings, G. K. *J. Am. Chem. Soc.* **2005**, *127*, 3048–3056; d) Gryparis, C.; Efe, C.; Raptis, C.; Lykakis, I. N.; Stratakis, M. *Org. Lett.* **2012**, *14*, 2956–2959; e) Neupane, P.; Xia, L.; Lee, Y. R. *Adv. Synth. Catal.* **2014**, *356*, 2566–2574.

(15) Fructos, M. R.; Belderrain, T. R.; Frémont, P.; Scott, N. M.; Nolan, S. P.; Díaz–Requejo, M. M.; Pérez, P. J. *Angew. Chem. Int. Ed.* **2005**, *44,* 5284–5288.

(16) Fructos, M. R.; De Fremont, P.; Nolan, S. P.; Diaz–Requejo, M. M.; Perez, P. J. *Organometallics* **2006**, *25*, 2237–2241.

(17) Anciaux, A. J.; Demonceau, A.; Noels, A. F.; Hubert, A. J.; Warin, R.; Teyssié, P. *J. Org. Chem.* **1981**, 46, 873–876.

(18) Díaz–Requejo, M. M.; Pérez, P. J. *Chem. Rev.* **2008**, *108*, 3379–3394.

(19) Doyle, M. P.; Duffy, R.; Ratnikov, M.; Zhou, L. *Chem. Rev.* **2010**, *110*, 704–724.

(20) Flores, J. A.; Komine, N.; Pal, K.; Pinter, B.; Pink, M.; Chen, C.–H.; Caulton, K. G.; Mindiola, D. J. *ACS Catal.* **2012**, *2*, 2066−2078.

(21) Paulissen, R.; Reimlinger, H.; Hayez, E.; Hubert, A. J.; Teyssié, P. *Tetrahedron Lett.* **1973**, *24*, 2233–2236.

(22) Liu, L.; Zhang, J. *Chem. Soc. Rev.* **2016**, *45*, 506–516.

(23) Fructos, M. R.; Belderrain, T. R.; Nicasio, M. C.; Nolan, S. P.; Kaur, H.; Díaz–Requejo, M. M.; Pérez, P. J. *J. Am. Chem. Soc.* **2004**, *126*, 10846–10847.

(24) Díaz–Requejo, M. M.; Belderraín, T. R.; Trofimenko, S.; Pérez, P. J. *J. Am. Chem. Soc.* **2001**, *123*, 3167–3168.

(25) a) Chen, Y.; Fields, K. B.; Zhang, X. P. *J. Am. Chem. Soc.* **2004**, *126*, 14718–14719; b) Chen, Y.; Ruppel, J. V.; Zhang, X. P. *J. Am. Chem. Soc.* **2007**, *129*, 12074–12075.

(26) a) Corma, A.; Serna, P.; Concepción, P.; Calvino, J. J. *J. Am. Chem. Soc.* **2008**, *130*, 8748–8753. For calculations see Ref. 31c.

(27) Wang, Z.; Bi, X.; Liao, P.; Zhang, R.; Liang, Y.; Dong, D., *Chem. Commun.* **2012**, *48*, 7076–7078.

(28) Kirmse, W. *Eur. J. Org. Chem.* **2002**, 2193–2256.

(29) a) Diaf, I.; Lemière, G.; Duñach, E. *Angew. Chem. Int. Ed.* **2014**, *53*, 4177–4180; b) Presset, M.; Coquerel, Y.; Rodriguez, J. *J. Org. Chem.* **2009**, *74*, 415–418.

(30) Shevchenko, V. V.; Shakhmin, A. A.; Nikolaev, V. A., *Russian J. Org. Chem.* **2006**, *42*, 1741–1744.

(31) a) Veschambre, H.; Vocelle, D. *Can. J. Chem.* **1969**, *47*, 1981–1988; b) Leyva, E.; Barcus, R. L.; Platz, M. S. *J. Am. Chem. Soc.* **1986**, 108, 7786–7788; c) Abad, A.; Corma, A.; García, H. *Chem. Eur. J.* **2008**, 14, 212– 222.

(32) a) Jadhav, A. M.; Bhunia, S.; Liao, H.–Y.; Liu, R.–S. *J. Am. Chem. Soc.* **2011**, *133*, 1769–1771; b) Li, X.; Incarvito, C. D.; Vogel, T.; Crabtree, R. H. *Organometallics* **2005**, *24*, 3066–3073; c) Bond, C. C.; Hooper, M. *J. Chem. Soc. C* **1969**, 2453–2460; d) Asao, N.; Sato, K.; Yamamoto, Y. *Tetrahedron Lett.* **2003**, 44, 5675–5677.

(33) Jin, H.; Tian, B.; Song, X.; Xie, J.; Rudolph, M.; Rominger, F.; Hashmi, A. S. K. *Angew. Chem. Int. Ed.* **2016**, *55*, 12688–12692.

TOC graphic